An optimization model for the treatment of perfluorocarboxylic acids considering membrane preconcentration and BDD electrooxidation.

Álvaro Soriano[a], Daniel Gorri[a], Lorenz T. Biegler[b], Ane Urtiaga[a]*

Affiliation:

[a]Department of Chemical and Biomolecular Engineering, University of Cantabria

Av. de Los Castros s/n. 39005 Santander. Spain

[b]Department of Chemical Engineering, Carnegie-Mellon University, Pittsburgh PA

15213-3890, U.S.A.

*Corresponding author: urtiaga@unican.es

Submitted to *Water Research*

July 2019

Abstract

Treatment of persistent perfluorocarboxylic acids in water matrixes requires of strong oxidation conditions, as those achieved by boron doped diamond (BDD) electrooxidation (ELOX). However, large scale implementation of ELOX is still hindered by its high energy consumption and economical investment. In this work, we used process systems engineering tools to define the optimal integration of a membrane pre-concentration stage followed by the BDD electrolysis of the concentrate, to drastically reduce the costs of treatment of perfluorohexanoic acid (PFHxA, 100 mg L^{-1}) in industrial waste streams. A multistage membrane cascade system using nanofiltration (NF90 and NF270 membranes) was considered to achieve more sophisticated PFHxA separations. The aim was to minimize the total costs by determining the optimal sizing of the two integrated processes (membrane area per stage and anode area) and the optimal process variables (pre-concentration operating time, electrolysis time, input and output concentrations). The non-linear programming model (NLP) was implemented in the General Algebraic Modelling System (GAMS). The results showed that for a *2-log* PFHxA abatement (99% removal), the optimal two membrane stages using the NF90 membrane obtains a 75.8% (6.4 \$ m^{-3}) reduction of the total costs, compared to the ELOX alone scenario (26.5 \$ m^{-3}). The optimized anode area and the energy savings, that were 85.3% and 88.2% lower than in ELOX alone, were the major contributions to the costs reduction. Similar results were achieved for a *3-log* and *4-log* PFHxA abatement, pointing out the promising benefits of integrating electrochemical oxidation with membrane pre-concentration through proper optimization for its large-scale application to waters impacted by perfluorocarboxylic acids.

Keywords: Electrooxidation; Membrane technology; Process optimization; Economic evaluation; Perfluoroalkyl substances (PFAS); Perfluorohexanoic acid (PFHxA)

1. Introduction

The growing presence of non-biodegradable and recalcitrant compounds in the environmental media and the inability of traditional wastewater treatment plants to remove this type of pollutants have forced researchers around the globe to find alternative treatment technologies (Sáez et al., 2013). Among them, electrochemical oxidation (ELOX) has gained a lot of attention as a promising technology for the mineralization or partial conversion of recalcitrant organic pollutants in wastewater (Anglada et al., 2009). ELOX may occur by two different mechanisms, direct oxidation and indirect oxidation, or a combination of both. Direct oxidation involves the diffusion of pollutants from the bulk of the liquid phase to the anode surface, followed by the direct electron transfer from the absorbed compounds. In indirect oxidation, the pollutant reacts in the liquid phase with electrogenerated oxidizing species, typically hydroxyl radicals (•OH), sulfate radicals and chlorine (Panizza and Cerisola, 2009).

The outstanding degradation capability of the ELOX technology is extended to the elimination of extremely recalcitrant perfluoroalkyl substances (Gomez-Ruiz et al., 2017). Per-and polyfluoroalkyl substances (PFASs) are a family of persistent man-made organic compounds that have been extensively used for the last half century in the manufacturing of a wide variety of products (Ross et al., 2018; Valsecchi et al., 2017). The growing concern about their bioaccumulation potential and ubiquitous

presence in the environment, especially of long-chain PFASs (number of $C \geq 7$), have led to limitations in their production and use, and extensive research is currently being performed about their treatment (Arvaniti and Stasinakis, 2015). Perfluorooctanesulfonic acid (PFOS) and perfluorooctanoic acid (PFOA) were incorporated into the European Union REACH regulation (The European Commission, 2017, 2010), with restrictions to their use and manufacture. Additionally, the USEPA has stablished PFOA and PFOS health advisory levels at 70 ng L^{-1} in drinking water (USEPA, 2016). Manufacturers are progressively phasing-out long-chain PFASs with their short-chain homologues and 6:2 fluorotelomers (Wang et al., 2013), also with high persistence properties (Brendel et al., 2018). Besides, 6:2 FTSA biodegradation pathways lead to short-chain perfluorocarboxylic acids, being PFHxA a major product (Zhang et al., 2016). Thus, growing concentrations of PFHxA in the environment are expected in the next years.

PFASs degradation by means of boron doped diamond (BDD) electrodes has been successfully applied at laboratory scale, achieving excellent defluorination and mineralization ratios in different concentration ranges and water matrixes, including industrial wastewater and groundwaters impacted by soil pollution (Gomez-Ruiz et al., 2018, 2017; Schaefer et al., 2017, 2015; Soriano et al., 2017; Urtiaga et al., 2015; Zhuo et al., 2012). However, a major drawback of electrochemical oxidation is the slow overall kinetics that results from mass transfer limitations in the low concentration range of PFASs (Pan et al., 2019). BDD electrodes also have the disadvantage of high chlorate and perchlorate generation, that, however, can be diminished working at low current densities (Urtiaga et al., 2018). Also, low

concentration of organics usually leads to low current efficiency, promoting undesirable secondary reactions such as the O_2 evolution reaction (Panizza et al., 2001). As a consequence, the high energy consumption of the ELOX technology (Anglada et al., 2010a; Gomez-Ruiz et al., 2017; Madsen et al., 2015) and the high economic investment when large electrode areas are needed (He et al., 2018; Radjenovic and Sedlak, 2015), make the large-scale practical implementation of electrooxidation for PFASs treatment an actual challenge.

The use of membrane separation processes could solve these limitations through the previous concentration of PFASs. On the one-hand, the higher concentration of organic compounds will boost the mass-transfer controlled kinetics of the electrolysis. Also, the natural content of dissolved salts will achieve higher concentrations, and the electrolyte will increase its electrical conductivity. As a result, the cell voltage of the electrochemical reactor will decrease, making the process less energy consuming (Bagastyo et al., 2012; Pérez et al., 2010). The higher concentration of electrolytes could also help to promote the electrochemical generation of oxidant species involved in degradation routes. Our previous experimental work (Soriano et al., 2017) reported the concentration of PFHxA from industrial process waters by means of nanofiltration, that was followed by the electrochemical degradation using BDD electrodes. The energy consumption of the electrolysis stage was estimated at 15.2 kWh m^{-3} for a 90% PFHxA abatement, a value that is significantly lower than the energy consumptions previously reported (Niu et al., 2016) for PFASs electrolysis. However, when more demanding PFHxA removals are needed, more sophisticated separations will be required, such as membrane cascade systems. Besides, a more

110 rigorous and not only energy-focused evaluation of the total economy of the
111 integrated process is also needed.

112 The rigorous design of a single-stage or multistage membrane pre-concentration
113 integrated to the ELOX process is a complex issue, as several variables regarding its
114 sizing and operation should be considered. The most relevant are the following: the
115 membrane area per stage, number of stages, the anode area, the pre-concentration
116 operating time, the electrolysis time, the concentrated volume to be electrolyzed as
117 well as the input and output concentration of solutes to the ELOX system and output
118 concentration of all solutes in the permeate and concentrate stream. They affect many
119 other variables, as the flowrates of the membrane system, the pumping and ELOX
120 system energy consumption, operating costs and capital investment costs. All these
121 variables are strongly interrelated and a trade-off between them should be established.
122 Additionally, the resulting hybrid process design must be less costly compared with
123 the application of the individual ELOX process alone. To design such complex cost-
124 optimal process it is necessary to use computer aided process engineering tools. The
125 formulated optimization problem must be solved by minimizing the total costs of the
126 integrated process, at the same time the optimal values of all the variables involved in
127 the process are calculated. To the best of our knowledge, this is the first time that
128 optimization models are used for the optimal integration of membrane and
129 electrochemical oxidation systems.

130 The novel approach proposed in this work is aimed at solving some of the challenges
131 for the implementation of ELOX technology. The case of study deals with the
132 treatment of persistent short chain perflurocarboxylic acids. More specifically, the

objective was set at the *2-log*, *3-log* and *4-log* reduction of PFHxA concentration in the treated water. We developed a semi-empirical mathematical model describing PFHxA concentration by means of a cascade of membrane elements and the BDD electrolysis of the concentrate stream obtained as retentate in the membrane system. We used optimization tools to determine the minimum total costs of the hybrid process, considering both the capital costs and the operating costs. To that end, optimal process sizing parameters and process variables were obtained for different target PFHxA concentrations at the end of the treatment train.

2. Methodology

2.1. *Description of the integrated process including membrane pre-concentration coupled to electrooxidation*

A schematic chart of the proposed membrane pre-concentration coupled to electrolysis system is illustrated in Fig. 1a. Both processes will be designed to work in sequential batch mode. First, the feed is sent to the pre-concentration (PC) membrane unit. At the end of the pre-concentration run time (t_{PC}), the volume of retentate that remains in the feed tank is used to feed the ELOX system. After the required electrolysis time (t_{ELOX}), the electrolyzed volume is mixed with the volume of permeate that was obtained in the membrane pre-concentration, resulting in the product volume. Transfer times are neglected. Each batch is processed once the precedent one has been completed.

The proposed membrane separation consists of a multistage cascade of membrane units where the permeate stream of the k stage is pressurized to become the feed to the k+1 stage (Fig. 1b). The successive filtration stages will allow to reduce the

concentration of pollutants in the permeate, that is finally collected in the permeate tank. The retentate stream of each stage is recycled to the previous stage, except the retentate from the first stage, that is recycled to the feed tank. In this way, the PFHxA concentration in the feed tank will increase over time. This multistage cascade design has been previously proposed for the separation of various chemicals when very high purities are demanded (Abejón et al., 2014, 2012; Caus et al., 2009). The characteristics of two nanofiltration membranes, NF90 and NF270 commercialized by Dow Filmtec, were considered for this study. Both membranes were previously tested at laboratory scale (Soriano et al., 2019a, 2019b) for the separation of PFHxA. The results showed that the NF90 membrane highly rejects PFHxA (rejection R>99%) but its water permeability is about one-half the permeability of the NF270 membrane, although the latter one achieved PFHxA rejections up to 95%. Ideally, the PFHxA concentration in the permeate should be as low as possible, although the membrane should be highly water-permeable, to diminish pre-concentration times and the costs related to the membrane system. Therefore, the evaluation of the NF90 and NF270 membranes in the different scenarios will help to identify the impact of the membrane selectivity/productivity trade-off on the optimal total cost of the hybrid process. Furthermore, the ELOX system is designed as a battery of n electrochemical reactors disposed in serial-parallel arrangement, all provided with boron-doped diamond electrodes (BDD). The design is based in the pilot plant that was built and tested by Anglada and coworkers (Anglada et al., 2010b) for the on-site treatment of landfill leachates.

178 Table 1 collects information about the problem input parameters such as operating
179 conditions, main characteristics of the hybrid process, and empirically obtained
180 parameters used to solve the optimization problem. We considered the PFHxA and
181 salts concentration in the feed water to be analogous to real industrial process waters
182 (Soriano et al., 2017)

183 *2.2. Process modelling*

184 The following assumptions were made when modelling the process.

185 • In the cascade membrane separation process, friction losses at the feed side of
186 the membrane element are neglected and, consequently, feed and retentate
187 pressure are the same. Therefore, the retentate is not pressurized when it is
188 recycled to the previous stage; however, the membrane permeate side is at
189 atmospheric pressure, and its pressure must be increased before feeding it to
190 the next membrane stage (Melin and Rautenbach, 2007).
191 • Membrane fouling was not considered and therefore membrane permeability
192 and the selectivity factor (α^i) will be used as constant parameters in the range
193 of concentration studied.
194 • All process streams are dilute aqueous solutions with the same constant
195 density.
196 • The residence time of the fluid inside the stack of electrochemical reactors is
197 negligible compared to its residence time in the recirculation tank.

198 *Modelling of the multistage membrane system*: Overall and component mass balances
199 for PFHxA and saline solutes in the feed and permeate tanks, assuming perfect
200 mixing, are written as follows,

$$\frac{dV_{ft}}{dt} = Q_{R,1} - Q_{ft} \quad (1)$$

$$\frac{dV_{pt}}{dt} = Q_{P,n} \quad (2)$$

$$\frac{d(V_{ft}\, C_{ft}^{i})}{dt} = Q_{R,1}\, C_{R,1}^{i} - Q_{ft}\, C_{ft}^{i} \quad (3)$$

$$\frac{d(V_{pt}\, C_{pt}^{i})}{dt} = Q_{P,n}\, C_{P,n}^{i} \quad (4)$$

201 The subscript *k*=1,2,…*n* refers to the number of the membrane stage. The superscript
202 *i* refers to the different compounds. The group of ordinary differential equations given
203 by Eqs (1)-(4) were discretized by Lagrange interpolation polynomials using Runge-
204 Kutta collocation methods in order to be solved as algebraic equations by GAMS
205 (Biegler, 2010).

206 The equivalent saline concentration in the feed tank was calculated according to Eq.
207 (5) (Pérez-González et al., 2015):

$$C_{eq} = 0.5 \sum_{i=1}^{s} |z^{i}|\, C_{ft}^{i} \quad (5)$$

208 The overall and solute mass balances in the mixers are written as follows:

209 *Stage 1*

$$Q_{ft} + Q_{R,2} = Q_{F,1} \quad (6)$$

$$Q_{ft}\, C_{ft}^{i} + Q_{R,2} C_{R,2}^{i} = Q_{F,1} C_{F,1}^{i} \quad (7)$$

Stage k

$$Q_{P,k-1} + Q_{R,k+1} = Q_{F,k} \quad (8)$$

$$Q_{P,k-1} C_{P,k-1}^{i} + Q_{R,k+1} C_{R,k+1}^{i} = Q_{F,k} C_{F,k}^{i} \quad (9)$$

Stage n

$$Q_{P,n-1} = Q_{F,n} \quad (10)$$

$$Q_{P,n-1} C_{P,n-1}^{i} = Q_{F,n} C_{F,n}^{i} \quad (11)$$

The overall and component *i* mass balances in the membrane modules are the following:

$$Q_{F,k} = Q_{R,k} + Q_{P,k} \quad (12)$$

$$Q_{F,k} C_{F,k}^{i} = Q_{R,k} C_{R,k}^{i} + Q_{P,k} C_{P,k}^{i} \quad (13)$$

The solute rejection factor at each membrane stage is defined as follows:

$$R^{i} = \left(1 - \frac{C_{P,k}^{i}}{C_{F,k}^{i}}\right) \times 100 \quad (14)$$

This equation can be rearranged to solve the solute mass transport across the membrane. Defining α^i=1-(R^i/100), we obtain the following relationship between the feed and the permeate solute concentration:

$$C_{P,k}^{i} = \alpha^{i} C_{F,k}^{i} \quad (15)$$

where α^i are empirically obtained selectivity parameters that are specific from each membrane and for every solute *i* (Table 1).

The permeate flowrate from membrane stage *k* is calculated using the modified Darcy's law expression, which considers the effective pressure gradient *(ΔP-Δπ)* across the membrane:

$$Q_{P,k} = 10^{-3}\, L_p\, A_k\, (\Delta P - \Delta\pi) \quad (16)$$

where L_p is the empirically determined membrane permeability (Soriano et al., 2019a, 2019b). The osmotic pressure difference (in psi) between both sides of the membrane is calculated according to Eq. (17) (Asano, 1998):

$$\pi = 1.19\, T \sum m^i \quad (17)$$

Modelling of the electrochemical reactor: The PFHxA mass balance in the ELOX recirculation tank is defined as follows,

$$\frac{dC_{ELOX}}{dt} = -k_{PFHxA} C_{ELOX} \frac{A_a}{V_{ELOX}} \quad (18)$$

where k_{PFHxA} is the PFHxA electrochemical degradation kinetic constant. Table 1 contains the empirically determined k_{PFHxA} value at 50 A m^{-2} in laboratory scale experiments (Soriano et al., 2017) using the BDD cell that is replicated in the design of the pilot plant. It should be noted that in Eq. (18) V_{ELOX} is the electrolyzed volume, which is equal to the volume of concentrate that was obtained in the membrane system at the end of the pre-concentration run ($V_{ELOX} = V_{ft}(t_{PC})$) and at t_{ELOX}=0, C_{ELOX} is equal to $C^{PFHxA}_{ft}(t_{PC})$.

From the mass balance at the mixing point we can calculate the required ELOX output concentration to meet the required PFHxA target concentration at the exit of the treatment train (Eq. (19)). Here, the target concentration will be defined by the desired PFHxA total abatement of the initial PFHxA concentration of fresh feed entering the process. In this work, we evaluated a *2-log* (99%), *3-log* (99.9 %) and *4-log* (99.99 %) reduction of the initial PFHxA concentration $C^{PFHxA}_{ft}(0)$.

$$C_{ELOX} = VRF\left[C_{target} - C_{pt}^{PFHxA}\left(1 - VRF^{-1}\right)\right] \quad (19)$$

In Eq. (19), *VRF* symbolizes the volume reduction factor in the pre-concentration run. *VRF* is the ratio between the initial feed volume and the final concentrate volume in the feed tank, at the end of the pre-concentration run. In the same way, we integrated Eq. (18) to define the required electrooxidation time to meet the demanded C_{ELOX}, Eq. (19), as a function of the pre-concentration time:

$$t_{ELOX} = \frac{ln\left[C_{ELOX}/C_{ft}^{PFHxA}(t_{PC})\right] V_{ELOX}}{-k_{PFHxA}\, A_a\, 60} \quad (20)$$

Where 60 is a factor (min h^{-1}) for the unit conversion of $k_{PFHxA.}$

2.3. Process economics

The hybrid process was optimized by determining the minimum total annual cost (TC), accounting for the capital expenditures (CAPEX) and the operating expenditures (OPEX):

$$TC = CAPEX\frac{r(1+r)^t}{(1+r)^t-1} + OPEX \quad (21)$$

In Eq. (21), the operating costs are on annual basis and the total capital investment is annualized taking into account the time value of money, being *T* the period of time and *r* the investment rate (Biegler et al., 1997). The fully detailed list of equations used for the estimation of capital and operating expenditures in Eq. (21) can be found in Table 2. The main parameters used in the process economics model are listed in Table 3.

We can also define the total specific cost (*TSC*) as the total annual cost related to the annual treated volume production (*AP*), the latter being defined as:

$$AP = \frac{OF}{t_{cycle}} V_{ft}(0) \quad (22)$$

with *OF* being the annual operation factor (Table 3) and t_{cycle} the cycle time needed to treat a single batch volume,

$$t_{cycle} = t_{PC} + t_{ELOX} \quad (23)$$

261 *2.4. Process optimization*

262 The full model described in Sections 2.2 and 2.3 can be formulated as the following
263 optimization problem statement:

$$\begin{aligned} &min\ TC(x) \\ &s.t\quad h(x)=0 \\ &\qquad g(x)\geq 0 \\ &\qquad L\leq x\leq U \end{aligned} \tag{37}$$

264 being x the vector of decision variables, h the vector of algebraic equations, g the
265 model constraints and L and U the lower and upper limits of the set of decision
266 variables.

267 We impose a *VRF* restriction, since reducing more than ten times the initial volume
268 in the pre-concentration process is not a technically realistic scenario:

$$VRF \leq 10 \tag{38}$$

269 We also restrict the membrane area per stage (A_k), by defining lower and upper bounds
270 to this variable based on the smallest and largest NF90 and NF270 membrane modules
271 that are commercialized (2.6 m^2 (4") and 37 m^2 (8")) (The Dow Chemical Company,
272 2013):

$$2.6 \leq A_k \leq 37 \tag{39}$$

273 Finally, and for the sake of comparison between different cases of study, we evaluated
274 the scenario in which the annual demand of volume of treated water (Eq. (22)), is
275 equal to 2000 $m^3\ y^{-1}$.

Thus, the herein presented optimization model is aimed at the minimization of the total annual cost (Eq. (21)) of the hybrid pre-concentration/electrooxidation process, for a required PFHxA abatement at the end of the treatment train and for a demanded annual volume production. For each abatement scenario, the optimal individual operating pre-concentration and electrooxidation times are obtained, as well as the sizing of each individual processes (i.e. the optimal total anode area and the membrane area per stage) and the output concentrations at the exit of the pre-concentration process, input and output concentrations at the ELOX system, energy consumption of both processes and capital and operating costs distributions. The dynamic nonlinear programing problem (NLP) was implemented in the General Algebraic Modelling System (GAMS) and solved using the IPOPTH solver on a 3.20 GHz Intel® Core™ i5-6500 processor.

3. Results and discussion

3.1. *Hybrid pre-concentration / electrooxidation process optimization results*

Table 4 and Table 5 show the optimal pre-concentration and electrooxidation times, membrane area per stage, anode electrode area and total cost for the different scenarios and for two types of nanofiltration membranes (NF270 and NF90), which differ in their water permeability and solute selectivity properties. We evaluated a *2-log*, *3-log* and *4-log* PFHxA elimination ratios at the exit of the process. We also evaluated 1, 2 and 3 pre-concentration stages in the membrane system and compared the total cost of all the scenarios with the application of ELOX alone without any pre-concentration stage. In Tables 4 and 5, a pre-concentration time equal to zero means

that the optimized solution eliminated the pre-concentration stage. This is the case of the NF270-1 stage integration for any target PFHxA removal ratio, and the NF90-1 stage integration for *3-log* and *4-log* PFHxA abatement. In these cases, the hybrid strategy does not bring any benefit from the point of view of total cost savings, since one membrane stage is not enough to obtain a high purity permeate. Since the required target concentration (C_{target}) is considerably lower than the permeate concentration (C^{PFHxA}_{pt}), the output ELOX concentration (C_{ELOX}) must be acutely low to meet the imposed mass balance at the exit of the treatment train. As a result, the ELOX energy costs are significantly higher, and the optimal solution eliminates the pre-concentration stage (t_{PC}=0), as it only contributes to increase the total treatment costs.

The distribution of all the optimal capital and operating costs, expressed as total specific cost, for the different cases of study are shown in Fig. 2 and Fig. 3, using the NF90 and the NF270 membrane, respectively. In all scenarios, the most important contribution to the total costs are the capital costs related to the electrochemical reactor system (from a 47% contribution in the worst scenario to a 36% impact in the best scenario). Based on the optimization results, the costs of the ELOX reactor can be greatly reduced though its integration with the membrane pre-concentration strategy, as the total anode area is significantly reduced. The membrane integration also managed to reduce all the operating costs related to the ELOX system, i.e, the lower the anode area, the lower are the costs related to the replacement of the anodes and maintenance. For the *2-log* PFHxA abatement, the anode area can be reduced from 9.1 m^2 in the case of only-ELOX, to 3.9 m^2 with NF90-1 stage integration, and furthermore, to 1.3 m^2 with NF90-2 membrane stages and 1.4 m^2 with NF90-3

membrane stages. This is translated into 51.3% savings of the total cost with the NF90-1 stage integration, compared to the application of the electrooxidation process alone. These savings are even higher with the use of 2 stages (75.8%) because of the lower optimal anode area capital and replacement costs. Overall, the integration results are slightly better when two membrane stages are used, since adding more membrane stages also increases the capital and operating costs related to the membrane system. On the other hand, cleaning costs only represents up to 0.9% of the total costs of the integrated process. In the case of cathode scaling promoters, such as calcium, being present at elevated concentrations, more frequent chemical cleanings will be needed. Nevertheless, due to the minor contribution of the cleaning costs to the total costs function the presence of scaling species would not have a great impact on the optimization results.

When an extremely demanding PFHxA abatement is required, as it is the *4-log* elimination scenario, the integration of a three stages membrane cascade provides better results, and the total savings increased to 78.4%, through the optimization of all the process variables. For the highly productive but more PFHxA permeable NF270 membrane, a *4-log* PFHxA abatement requires a three stages cascade pre-concentration, although the total cost is slightly higher than for the NF90 integration. This is because the optimal output ELOX concentration in the NF270 integration scenario (C_{ELOX}=0.02 mg L^{-1}) is more demanding than when using the NF90 (C_{ELOX}=0.1 mg L^{-1}), which, as previously explained, is a consequence of the lower PFHxA rejection of the NF270 membrane. As a consequence, the costs related to the ELOX energy consumption are higher. As the ELOX capital costs clearly overshadow

345 the membrane system equipment costs, it is possible to add up to three membrane
346 stages for a *4-log* abatement and still get a slight reduction of the total costs. (e.g, in
347 the *4-log* NF90 case of study). In general, the membrane equipment investment only
348 represents 7% to 13% of the total costs in those scenarios in which the integration
349 approach works, and the pump capital cost contributions are up to 7%.

350 The integration strategy is also able to accomplish important reductions on the
351 operating costs related to the energy consumption of the process compared to the
352 application of the electrolysis alone. Depending on the PFHxA elimination target, the
353 energy specific costs of the only-ELOX scenario range from 4.7 \$ m^{-3} for a *2-log*
354 PFHxA removal to 9.4 \$ m^{-3} for a *4-log* removal. Remarkably, the membrane coupling
355 approach can reduce the energy costs to 0.6 \$ m^{-3}, 0.7 \$ m^{-3} and 1.0 \$ m^{-3} for a *2-log*,
356 *3-log* and *4-log* PFHxA abatement, respectively. These energy savings (up to 89%)
357 notably impact the total costs, as the energy cost contribution to the total costs is
358 reduced from a 18% to only 8-9%. The pathway for reducing the energy costs goes
359 through the optimization of the electrolysis time, which is much lower in the
360 membrane integrated system than in the approach with ELOX alone. The cutback on
361 the electrolysis time is mainly due to (i) the much lower volume to be electrolyzed
362 and, (ii) the less demanding PFHxA concentration at the exit of the ELOX system that
363 is needed to meet the target concentration at the exit of the treatment train (Eq. (19)).
364 This is also influenced by the very low PFHxA concentration obtained in the permeate
365 tank of the membrane system at the end of the pre-concentration run. Additionally,
366 membrane separation also increases the concentration of salts in solution, to make the
367 electrolyte more conductive, and therefore the cell voltage is also reduced,

368 diminishing to a lesser degree the ELOX energy costs. As Fig. 4 shows, the ELOX
369 energy savings have a huge impact on the overall energy consumption. Taking as a
370 reference the estimated electrolysis energy consumptions of the ELOX-only scenario
371 (29.3 kWh m^{-3}, 43.9 kWh m^{-3} and 58.5 kWh $m^{-3,}$ for a *2-log*, *3-log* and *4-log* PFHxA
372 abatement, respectively) the optimized hybrid process consumes 29.3% – 89.7% less
373 energy, depending on the type of membrane used and on the number of membrane
374 stages. In most cases, and except for the *2-log* NF90-1 stage scenario, the use of a
375 single membrane stage does not provide energy savings.

376 *3.2. Parametric sensitivity analysis*

377 The two commercial membranes considered in this work (NF90 and NF270) yielded
378 excellent results in the integrated process through proper optimization of the process
379 variables. However, it is interesting to determine if hypothetically more selective or
380 more permeable membrane materials would achieve better results in terms of
381 minimization of the total costs. It should be also highlighted that the rejection
382 performance of the herein studied membranes can be affected by the increase of the
383 solution ionic strength, pH acidification or due to the effect of concentration on the
384 selectivity factor. Initial permeate flux might also be reduced as a consequence of
385 organic and inorganic fouling. Hence, in this section, a sensitivity analysis is
386 performed with the aim of getting a deeper understanding on the influence of the
387 studied membrane properties on the total cost objective function. Additionally, we
388 evaluated the influence of the kinetic constant of the electrochemical PFHxA
389 degradation on the total costs objective function when using the NF90 membrane and
390 different number of membrane stages.

The effect of the membrane hydraulic permeability (L_p) and the selectivity factor (α^{PFHxA}) on the total specific cost for a *3-log* PFHxA abatement is shown in Fig. 5. Only two and three membrane stages are illustrated since the use of a single membrane stage did not provide any optimal TSC below the only-ELOX scenario. In Fig. 5, the dark red area corresponds to TSC solutions in which the optimal scenario is to eliminate the pre-concentration process and therefore, the integration does not provide any advantage. For orientation purposes, the optimal results of the two commercial membranes studied in this work (NF90 and NF270) have been added to the figure, according to their PFHxA selectivity and hydraulic permeability data (Table 1). In Fig. 5, α^{PFHxA} ranges from α^{PFHxA} =0.1 (equivalent to R_{PFHxA}=90%) to α^{PFHxA}=0.005 (R_{PFHxA}=99.5%), since the empirical values of PFHxA rejection ranged from 94.8% (NF270) and 99.4% (NF90).

In Figures 5a and 5b, the lower left hand corner would correspond to TSC solutions theoretically given by reverse osmosis membranes typically characterized by their low permeability and very high selectivity (low α^{PFHxA} value) (Soriano et al., 2019a). With two membrane stages (Fig 5a), only membranes with very high PFHxA selectivity and medium-high water permeability would be able to accomplish significant total cost savings, as in the case of the NF90 membrane. However, as seen in Fig. 5a the excellent results given by the NF90 membrane are subject to changes in the optimum TSC with any hypothetical reduction of the PFHxA rejection performance or by any decrease of the membrane permeate flux as a result of membrane fouling.

On the other hand, less selective but more water permeable membranes, such as the NF270, achieve similar total costs savings when three membrane stages are considered (Fig 5b). In contrast with the 2-stage integration scenario, any rejection decline in the 3-stage integration scenario would not severally affect the optimal TSC given by the two nanofiltration membranes. However, from a process operation viewpoint it is easier and more suitable to manage a process with fewer membrane stages. Also, according to Fig. 5, more selective and more productive membranes would be able to reduce the TSC to a minimum of 7.2 \$ m^{-3}, which is very close to the best scenario obtained with the commercial NF90 membrane and by means of two membrane stages (8.3 \$ m^{-3}). Finally, in any integration scenario the use of highly PFHxA selective but low water-permeable membranes, as in the case of some reverse osmosis membranes, is not recommended, as any noticeable reduction of the PFHxA rejection performance would severally modify the optimal TSC, thus compromising the benefits of the integrated strategy. It is also worth mentioning that literature reports effective nanofiltration retentions of shorter-chained PFASs such as perfluorobutanoic acid (PFBA), perfluorobutanesulfonic acid (PFBS) and perfluoropentanoic acid (PFPeA), that are generally above 93-95% (Appleman et al., 2013; Steinle-Darling and Reinhard, 2008). From Fig.5, it can be seen that the use of the NF-ELOX strategy for the treatment of these substances may require up to 3 stages to bring benefits from the point of view of total costs savings.

Fig. 6 shows the sensibility of the optimized solution to variations of the kinetics of PFHxA electrolysis. Considering a *3-log* PFHxA abatement and using the NF90, doubling the value of k_{PFHxA} (Table 1) would reduce the total costs of the hybrid

process from 8.3 \$ m^{-3} to 5.5 \$ m^{-3}, a consequence of the drastic 45% reduction of the optimal anode area. Conversely, halving the value of k_{PFHxA} has a greater impact on the objective function, as the total costs are elevated to 13.4 \$ m^{-3}. Yet, in this hypothetical scenario the integrated strategy would be still able to reduce the total costs a remarkable 65.3% compared to the application of the electrooxidation alone without previous pre-concentration.

4. Conclusions

This work demonstrates the advantages of integrating membrane separation with electrochemical oxidation for the treatment of short chain perfluorocarboxylic acids (PFCAs) in polluted waters. This novel approach uses process systems engineering tools to optimize the process variables in order to minimize the total costs of the process. Particularly, we studied the treatment of perfluorohexanoic acid at concentration levels that are found in industrial process waters (100 mg L^{-1}).

The results from this work shows that it is possible to achieve important savings in the total costs of the electrochemical treatment of persistent PFCAs through its integration with membrane pre-concentration. Moreover, through rigorous optimization, the integrated membrane separation-electrooxidation process is able to fulfil highly demanding pollutant abatement requirements, in a much less costly way compared to the application of electrooxidation alone. Overall, elimination objectives are satisfied just with a two-stage membrane pre-concentration layout, achieving excellent savings of the process total costs (up to 78.4%). Overall, it is economically preferable to use nanofiltration membranes, characterized by their medium to high hydraulic permeability and medium to high PFHxA selectivity, in

459 opposition to low permeable and highly selective reverse osmosis membranes. Still,
460 even in the best optimal integration scenarios, which allow 86% reduction of the
461 electrochemical reactor anodic area, the costs related to investment, replacement and
462 maintenance of the electrodes, clearly outweigh the rest of the process capital and
463 operating costs. BDD electrodes achieves outstanding performance for degradation,
464 mineralization, and defluorination of perfluorinated compounds. Despite the
465 excellent results achieved by the integrated process, the high price of the BDD
466 electrodes remains as a bottleneck in the actual implementation of large-scale
467 electrochemical processes. Thus, research efforts should be directed towards the
468 optimization of the BDD manufacturing process or towards the development of new
469 cheaper but equally effective electrocatalytic materials.

470

471 **Acknowledgments**

472 Financial support by the Spanish Ministry of Economy and Business through the
473 projects CTM2016-75509-R and CTQ2016-75158-R (MINECO, SPAIN-FEDER
474 2014–2020) is gratefully acknowledged.

475

Nomenclature

A_e	Total anode electrode area (m^2)
A_k	Stage k membrane area (m^2)

$CAPEX$	Total capital expenses ($)
CC_{ELOX}	Electrooxidation plant capital expenses ($)
C_{clean}	Cleaning operating costs ($ y^{-1})
CC_M	Membrane equipment capital cost ($)
CC_p	Pre-concentration pumping capital cost ($)
C_{ELOX}	Concentration in the ELOX reactor (mg L^{-1})
C_{energy}	Energy costs ($ y^{-1})
C_{eq}	Equivalent ion concentration (mol L^{-1})
C_{erep}	Electrode replacement costs ($ y^{-1})
$C^i_{F,k}$	Feed stream to stage k solute concentration (mg L^{-1})
C^i_{ft}	Solute concentration in the feed tank (mg L^{-1})
C_{maint}	Maintenance operating costs ($ y^{-1})
C_{mrep}	Membrane replacement costs ($ y^{-1})
$C^i_{P,k}$	Stage k permeate stream solute concentration (mg L^{-1})
C^i_{pt}	Permeate tank solute concentration (mg L^{-1})
$C^i_{R,k}$	Retentate stream solute concentration (mg L^{-1})
C_{target}	PFHxA target concentration (mg L^{-1})
E_{ELOX}	ELOX energy consumption (kWh)

EL	Electrode material life (y)
EP	Electrode material price ($ m^{-2})
E_{PC}	NF energy consumption (kWh)
f_1	Material pump factor
f_2	Suction pressure factor
J_{app}	Current density (A m^{-2})
k_{PFHxA}	PFHxA degradation kinetic constant (m min^{-1})
L	Pumps labor factor
L_p	Membrane permeability (L m^{-2} h^{-1} bar^{-1})
m^i	Molality of the species dissolved (mol kg^{-1})
ML	Membrane module life (y)
MMP	Membrane module price ($ m^{-2})
OF	Operating factor (h y^{-1})
$OPEX$	Operating expenses ($ y^{-1})
P_{ELOX}	Electrooxidation power supply (kW)
$Q_{F,k}$	Feed flow rate to stage k (m^3 h^{-1})
Q_{ft}	Volumetric flow rate from feed tank (m^3 h^{-1})
$Q_{P,k}$	Permeate volumetric flow rate from stage k ($m^3.h^{-1}$)
$Q_{R,k}$	Retentate volumetric flow rate from stage k (m^3 h^{-1})

r	Investment rate (%)
R^i	Rejection of solute i
T	Temperature of the solution (K)
t	Period (y)
TC	Total annual cost ($\$\ y^{-1}$)
TSC	Total specific cost ($\$\ m^{-3}$)
$tcycle$	Cycle time (h)
t_{ELOX}	ELOX operation time (h)
t_{PC}	Pre-concentration time (h)
U	ELOX cell voltage (V)
V_{ft}	Feed tank volume (m^3)
V_{pt}	Permeate tank volume (m^3)
VRF	Volume reduction factor (-)
z^i	Ionic valence (-)
α^i	Solute partitioning empirical parameter (-)
ΔP	Effective pressure difference (bar)
$\Delta\pi$	Osmotic pressure difference (bar)
η	Pump efficiency (%)
π	Osmotic pressure (bar)

476

477 **References**

478 Abejón, R., Garea, A., Irabien, A., 2014. Analysis and optimization of continuous organic
479 solvent nanofiltration by membrane cascade for pharmaceutical separation. AIChE
480 J. 60, 931–948. doi:10.1002/aic.14345

481 Abejón, R., Garea, A., Irabien, A., 2012. Integrated countercurrent reverse osmosis
482 cascades for hydrogen peroxide ultrapurification. Comput. Chem. Eng. 41, 67–76.
483 doi:10.1016/j.compchemeng.2012.02.017

484 Anglada, A., Ortiz, D., Urtiaga, A.M., Ortiz, I., 2010a. Electrochemical oxidation of
485 landfill leachates at pilot scale: Evaluation of energy needs. Water Sci. Technol. 61,
486 2211–2217. doi:10.2166/wst.2010.130

487 Anglada, A., Urtiaga, A., Ortiz, I., 2009. Contributions of electrochemical oxidation to
488 waste-water treatment: Fundamentals and review of applications. J. Chem. Technol.
489 Biotechnol. 84, 1747–1755. doi:10.1002/jctb.2214

490 Anglada, A., Urtiaga, A.M., Ortiz, I., 2010b. Laboratory and pilot plant scale study on
491 the electrochemical oxidation of landfill leachate. J. Hazard. Mater. 181, 729–735.
492 doi:10.1016/j.jhazmat.2010.05.073

493 Appleman, T.D., Dickenson, E.R. V, Bellona, C., Higgins, C.P., 2013. Nanofiltration and
494 granular activated carbon treatment of perfluoroalkyl acids. J. Hazard. Mater. 260,
495 740–746.

496 Arkell, A., Krawczyk, H., Thuvander, J., Jönsson, A.S., 2013. Evaluation of membrane
497 performance and cost estimates during recovery of sodium hydroxide in a
498 hemicellulose extraction process by nanofiltration. Sep. Purif. Technol. 118, 387–
499 393. doi:10.1016/j.seppur.2013.07.015

500 Arvaniti, O.S., Stasinakis, A.S., 2015. Review on the occurrence, fate and removal of
501 perfluorinated compounds during wastewater treatment. Sci. Total Environ. 524–
502 525, 81–92. doi:10.1016/j.scitotenv.2015.04.023

503 Asano, T., 1998. Wastewater Reclamation and Reuse: Water Quality Management
504 Library. CRC Press, Florida.

505 Bagastyo, A.Y., Batstone, D.J., Kristiana, I., Gernjak, W., Joll, C., Radjenovic, J., 2012.
506 Electrochemical oxidation of reverse osmosis concentrate on boron-doped diamond
507 anodes at circumneutral and acidic pH. Water Res. 46, 6104–6112.
508 doi:10.1016/j.watres.2012.08.038

509 Biegler, L.T., 2010. Nonlinear Programming: Concepts, Algorithms and Applications to
510 Chemical Processes. Society for Industrial and Applied Mathematics, Philadelphia.

511 Biegler, L.T., Grossmann, I.E., Westerberg, A.W., 1997. Systematic methods of chemical
512 process design. Prentice Hall PTR, New Jersey.

513 Brendel, S., Fetter, É., Staude, C., Vierke, L., Biegel-Engler, A., 2018. Short-chain
514 perfluoroalkyl acids: environmental concerns and a regulatory strategy under
515 REACH. Environ. Sci. Eur. 30, 9. doi:10.1186/s12302-018-0134-4

516 Cañizares, P., Paz, R., Sáez, C., Rodrigo, M.A., 2009. Costs of the electrochemical

517 oxidation of wastewaters: A comparison with ozonation and Fenton oxidation
518 processes. J. Environ. Manage. 90, 410–420. doi:10.1016/j.jenvman.2007.10.010

519 Caus, A., Braeken, L., Boussu, K., Van der Bruggen, B., 2009. The use of integrated
520 countercurrent nanofiltration cascades for advanced separations. J. Chem. Technol.
521 Biotechnol. 84, 391–398. doi:10.1002/jctb.2052

522 Eurostat, 2018. Electricity price statistics [WWW Document]. URL
523 https://ec.europa.eu/eurostat/statistics-
524 explained/index.php/Electricity_price_statistics (accessed 10.29.18).

525 Gomez-Ruiz, B., Diban, N., Urtiaga, A., 2018. Comparison of microcrystalline and
526 ultrananocrystalline boron doped diamond anodes: Influence on perfluorooctanoic
527 acid electrolysis. Sep. Purif. Technol. 208, 169–177.
528 doi:10.1016/j.seppur.2018.03.044

529 Gomez-Ruiz, B., Gómez-Lavín, S., Diban, N., Boiteux, V., Colin, A., Dauchy, X.,
530 Urtiaga, A., 2017. Efficient electrochemical degradation of poly- and perfluoroalkyl
531 substances (PFASs) from the effluents of an industrial wastewater treatment plant.
532 Chem. Eng. J. 322, 196–204. doi:10.1016/j.cej.2017.04.040

533 He, Y., Lin, H., Guo, Z., Zhang, W., Li, H., Huang, W., 2018. Recent developments and
534 advances in boron-doped diamond electrodes for electrochemical oxidation of
535 organic pollutants. Sep. Purif. Technol. 212, 802–821.
536 doi:10.1016/j.seppur.2018.11.056

537 Kraft, A., 2007. Doped Diamond: A Compact Review on a New, Versatile Electrode

538 Material. Int. J. Electrochem. Sci. 2, 335–338.

539 Madsen, H.T., Søgaard, E.G., Muff, J., 2015. Reduction in energy consumption of
540 electrochemical pesticide degradation through combination with membrane
541 filtration. Chem. Eng. J. 276, 358–364. doi:10.1016/j.cej.2015.04.098

542 Martínez-Huitle, C.A.C.A., Rodrigo, M.A.M.A., Sirés, I., Scialdone, O., 2015. Single and
543 Coupled Electrochemical Processes and Reactors for the Abatement of Organic
544 Water Pollutants: A Critical Review. Chem. Rev. 115, 13362–13407.
545 doi:10.1021/acs.chemrev.5b00361

546 Melin, T., Rautenbach, R., 2007. Membranverfahren. Grundlagen der Modul- und
547 Anlagenauslegung. Springer, Berlin.

548 Niu, J., Li, Y., Shang, E., Xu, Z., Liu, J., 2016. Electrochemical oxidation of
549 perfluorinated compounds in water. Chemosphere 146, 526–538.
550 doi:10.1016/j.chemosphere.2015.11.115

551 Pan, Z., Song, C., Li, L., Wang, H., Pan, Y., Wang, C., Li, J., Wang, T., Feng, X., 2019.
552 Membrane technology coupled with electrochemical advanced oxidation processes
553 for organic wastewater treatment: recent advances and future prospects. Chem. Eng.
554 J. doi:10.1016/j.cej.2019.01.188

555 Panizza, M., Cerisola, G., 2009. Direct and mediated anodic oxidation of organic
556 pollutants. Chem. Rev. 109, 6541–6569. doi:10.1021/cr9001319

557 Panizza, M., Michaud, P.A., Cerisola, G., Comninellis, C., 2001. Anodic oxidation of 2-
558 naphthol at boron-doped diamond electrodes. J. Electroanal. Chem. 507, 206–214.

559 doi:10.1016/S0022-0728(01)00398-9

560 Pérez-González, A., Ibáñez, R., Gómez, P., Urtiaga, A.M., Ortiz, I., Irabien, J.A., 2015.
561 Nanofiltration separation of polyvalent and monovalent anions in desalination
562 brines. J. Memb. Sci. 473, 16–27.
563 doi:http://dx.doi.org/10.1016/j.memsci.2014.08.045

564 Pérez, G., Fernández-Alba, A.R., Urtiaga, A.M., Ortiz, I., 2010. Electro-oxidation of
565 reverse osmosis concentrates generated in tertiary water treatment. Water Res. 44,
566 2763–2772. doi:http://dx.doi.org/10.1016/j.watres.2010.02.017

567 Radjenovic, J., Sedlak, D.L., 2015. Challenges and Opportunities for Electrochemical
568 Processes as Next-Generation Technologies for the Treatment of Contaminated
569 Water. Environ. Sci. Technol. 49, 11292–11302. doi:10.1021/acs.est.5b02414

570 Ross, I., McDonough, J., Miles, J., Storch, P., Thelakkat Kochunarayanan, P., Kalve, E.,
571 Hurst, J., S. Dasgupta, S., Burdick, J., 2018. A review of emerging technologies for
572 remediation of PFASs. Remediat. J. 28, 101–126. doi:10.1002/rem.21553

573 Sabatino, S., Galia, A., Saracco, G., Scialdone, O., 2017. Development of an
574 Electrochemical Process for the Simultaneous Treatment of Wastewater and the
575 Conversion of Carbon Dioxide to Higher Value Products. ChemElectroChem 4,
576 150–159. doi:10.1002/celc.201600475

577 Sáez, C., Cañizares, P., Llanos, J., Rodrigo, M.A., 2013. The Treatment of Actual
578 Industrial Wastewaters Using Electrochemical Techniques. Electrocatalysis 4, 252–
579 258. doi:10.1007/s12678-013-0136-3

580 Schaefer, C.E., Andaya, C., Burant, A., Condee, C.W., Urtiaga, A., Strathmann, T.J.,
581 Higgins, C.P., 2017. Electrochemical treatment of perfluorooctanoic acid and
582 perfluorooctane sulfonate: insights into mechanisms and application to groundwater
583 treatment. Chem. Eng. J. 317, 424–432. doi:10.1016/j.cej.2017.02.107

584 Schaefer, C.E., Andaya, C., Urtiaga, A., McKenzie, E.R., Higgins, C.P., 2015.
585 Electrochemical treatment of perfluorooctanoic acid (PFOA) and perfluorooctane
586 sulfonic acid (PFOS) in groundwater impacted by aqueous film forming foams
587 (AFFFs). J. Hazard. Mater. 295, 170–175. doi:10.1016/j.jhazmat.2015.04.024

588 Sethi, S., Wiesner, M.R., 2000. Cost modelling and estimation of crossflow membrane
589 filtration processes. Environ. Eng. Sci. 17, 61–79.

590 Soriano, Á., Gorri, D., Urtiaga, A., 2019a. Selection of High Flux Membrane for the
591 Effective Removal of Short-Chain Perfluorocarboxylic Acids. Ind. Eng. Chem. Res.
592 58, 3329–3338. doi:10.1021/acs.iecr.8b05506

593 Soriano, Á., Gorri, D., Urtiaga, A., 2019b. Membrane preconcentration as an efficient
594 tool to reduce the energy consumption of perfluorohexanoic acid electrochemical
595 treatment. Sep. Purif. Technol. 208, 160–168. doi:10.1016/j.seppur.2018.03.050

596 Soriano, Á., Gorri, D., Urtiaga, A., 2017. Efficient treatment of perfluorohexanoic acid
597 by nanofiltration followed by electrochemical degradation of the NF concentrate.
598 Water Res. 112, 147–156. doi:10.1016/j.watres.2017.01.043

599 Steinle-Darling, E., Reinhard, M., 2008. Nanofiltration for trace organic contaminant
600 removal: Structure, solution, and membrane fouling effects on the rejection of

perfluorochemicals. Environ. Sci. Technol. 42, 5292–5297.

The Dow Chemical Company, 2013. Water & Process Solutions, FILMTEC ™ Reverse Osmosis Membranes: Technical Manual.

The European Commission, 2017. Commission Regulation (EU) 2017/1000 of 13 June 2017: Amending Annex XVII to Regulation (EC) No 1907/ 2006 of the European Parliament and of the Council concerning the Registration, Evaluation, Authorisation and Restriction of Chemicals (REACH) as regard. Off. J. Eur. Union L 150, 14–18.

The European Commission, 2010. Commission Regulation (EU) No 757/2010 of 24 August 2010 amending Regulation (EC) No 850/2004 of the European Parliament and of the Council on persistent organic pollutants as regards Annexes I and III Text with EEA relevance. Off. J. Eur. Union L 223, 29–36.

Urtiaga, A., Fernández-González, C., Gómez-Lavín, S., Ortiz, I., 2015. Kinetics of the electrochemical mineralization of perfluorooctanoic acid on ultrananocrystalline boron doped conductive diamond electrodes. Chemosphere 129, 20–26. doi:10.1016/j.chemosphere.2014.05.090

Urtiaga, A., Soriano, A., Carrillo-Abad, J., 2018. BDD anodic treatment of 6:2 fluorotelomer sulfonate (6:2 FTSA). Evaluation of operating variables and by-product formation. Chemosphere 201, 571–577. doi:10.1016/j.chemosphere.2018.03.027

USEPA, 2016. Drinking Water Health Advisories for PFOA and PFOS [WWW

622 Document]. URL https://www.epa.gov/ground-water-and-drinking-water/drinking-
623 water-health-advisories-pfoa-and-pfos (accessed 3.16.18).

624 USEPA, 2006. Technology and Cost Document for the Final Ground Water Rule [WWW
625 Document]. URL
626 https://nepis.epa.gov/Exe/ZyPDF.cgi/P1002Y6I.PDF?Dockey=P1002Y6I.PDF
627 (accessed 5.6.19).

628 Valsecchi, S., Conti, D., Crebelli, R., Polesello, S., Rusconi, M., Mazzoni, M., Preziosi,
629 E., Carere, M., Lucentini, L., Ferretti, E., Balzamo, S., Simeone, M.G., Aste, F.,
630 2017. Deriving environmental quality standards for perfluorooctanoic acid (PFOA)
631 and related short chain perfluorinated alkyl acids. J. Hazard. Mater. 323, 84–98.
632 doi:10.1016/j.jhazmat.2016.04.055

633 Vince, F., Marechal, F., Aoustin, E., Bréant, P., 2008. Multi-objective optimization of
634 RO desalination plants. Desalination 222, 96–118. doi:10.1016/j.desal.2007.02.064

635 Wang, Z., Cousins, I.T., Scheringer, M., Hungerbühler, K., 2013. Fluorinated alternatives
636 to long-chain perfluoroalkyl carboxylic acids (PFCAs), perfluoroalkane sulfonic
637 acids (PFSAs) and their potential precursors. Environ. Int. 60, 242–248.
638 doi:10.1016/j.envint.2013.08.021

639 Zarca, G., Urtiaga, A., Biegler, L.T., Ortiz, I., 2018. An optimization model for
640 assessment of membrane-based post-combustion gas upcycling into hydrogen or
641 syngas. J. Memb. Sci. 563, 83–92. doi:10.1016/j.memsci.2018.05.038

642 Zhang, S., Lu, X., Wang, N., Buck, R.C., 2016. Biotransformation potential of 6:2

643 fluorotelomer sulfonate (6:2 FTSA) in aerobic and anaerobic sediment.
644 Chemosphere 154, 224–230. doi:10.1016/j.chemosphere.2016.03.062

645 Zhuo, Q., Deng, S., Yang, B., Huang, J., Wang, B., Zhang, T., Yu, G., 2012. Degradation
646 of perfluorinated compounds on a boron-doped diamond electrode. Electrochim.
647 Acta 77, 17–22. doi:10.1016/j.electacta.2012.04.145

648

649

650 **Table 1.** Process model input parameters.

Initial conditions	
Initial concentration of solutes in the feed tank, C^i_{ft}	
PFHxA	100 mg L^{-1}
SO_4^{2-}	338 mg L^{-1}
Na^+	162 mg L^{-1}
Feed and permeate tanks volume	
V_{ft} *(0)*	10 m^3
V_{pt} *(0)*	0 m^3
Operating conditions and process parameters	
Operating feed pressure at each membrane stage *k*	10 bar
Flow rate from feed tank to cascade membrane system, Q_{ft}	3.2 m^3 h^{-1}
Solution temperature, *T*	293 K
ELOX current density, J_{app}	50 A m^{-2}
Empirical parameters (Soriano et al., 2019b, 2019a, 2017)	
Membrane hydraulic permeability	
NF90 permeability, $L_{p,\,NF90}$	6.98 L m^{-2} h^{-1} bar^{-1}
NF270 permeability, $L_{p,\,NF270}$	9.40 L m^{-2} h^{-1} bar^{-1}
NF90 solute transport correlation factor	
α^{PFHxA}	0.0066
$\alpha^{SO_4^{2-}}$	0.0129
α^{Na^+}	0.0152
NF270 solute transport correlation factor	
α^{PFHxA}	0.0520
$\alpha^{SO_4^{2-}}$	0.0369
α^{Na^+}	0.3228
ELOX cells empirical data	
PFHxA degradation kinetic constant at J_{app} = 50 A m^{-2}, k_{PFHxA}	0.0021 m min^{-1}

651

652

653 **Table 2**. Process economics equations used for the estimation of capital and operating costs in Eq.
654 (21).
655

Capital costs
Total capital costs
$CAPEX = CC_M + CC_{ELOX} + CC_P$ (24)
Membrane equipment capital costs including membrane housing (Abejón et al., 2012; USEPA, 2006)
$CC_M = \left(MMP \sum_{k=1}^{n} A_k \right) + V_{pt}(t_{PC}) 14.85 \frac{24}{t_{cycle}}$ (25)
Electrooxidation equipment capital costs (Cañizares et al., 2009)
$CC_{ELOX} = 19216 \left({A_e}^{0.7857} \right) + 9000\, A_e + 0.25\, P_{ELOX}$ (26)
Pump capital costs (Sethi and Wiesner, 2000)
$CC_P = 81.27\, UF\, f_1\, f_2\, L \left[(Q_{ft}\, \Delta P)^{0.39} + \left(\sum_{k=1}^{n-1} Q_{P,k}\, \Delta P \right)^{0.39} \right]$ (27)
Operating costs
Total operating costs
$OPEX = C_{clean} + C_{maint} + C_{mrep} + C_{erep} + C_{energy}$ (28)
Cleaning costs (Arkell et al., 2013; USEPA, 2006)
$C_{clean} = 50 \times A_e + 2.63 \times 10^{-3}\, V_{pt}(t_{PC}) \frac{OF}{t_{cycle}}$ (29)
Maintenance costs (Arkell et al., 2013)
$C_{maint} = 0.02\, CAPEX$ (30)
Membrane replacement costs (Abejón et al., 2012)
$C_{mrep} = \frac{MMP}{ML} \sum_{k=1}^{n} A_k$ (31)
Electrode replacement costs
$C_{erep} = \frac{EP}{EL} A_e$ (32)
Energy costs (Zarca et al., 2018)
$C_{energy} = ElP\, (E_{ELOX} + E_{PC})\, \frac{OF}{t_{cycle}}$ (33)
Electrooxidation process energy consumption (Martínez-Huitle et al., 2015)
$E_{ELOX} = 10^{-3}\, U\, J_{app}\, A_e\, t_{ELOX}$ (34)
Equivalent saline concentration – ELOX cell voltage empirical correlation (Soriano et al., 2019b)
$U = 11.649\, (C_{eq} - 5.65 \times 10^{-3})^{-4.84 \times 10^{-2}}$ (35)
Pre-concentration process pumping energy consumption
$E_{PC} = \frac{\Delta P\, t_{PC}}{36\, \eta} \left(\sum_{k=1}^{n-1} Q_{p(k)} + Q_{ft} \right)$ (36)

656

657 **Table 3**. Economic model process parameters.

Parameter	**Value**
Investment rate, *r* (Zarca et al., 2018)	10%
Period, *T* (Zarca et al., 2018)	15 y
Pump construction material factor, f_1 (ductile iron) (Sethi and Wiesner, 2000)	1
Suction pressure range factor, f_2 (suction pressures up to 150 psi) (Sethi and Wiesner, 2000)	1
Labor factor, *L* (Sethi and Wiesner, 2000)	1.4
Membrane equipment price, *MMP*	500 \$ m^{-2}
Membrane module life, *ML*	8 y
BDD anode electrode price, *EP* (Cañizares et al., 2009; Sabatino et al., 2017)	9000 \$ m^{-2}
BDD anode electrode expected life, *EL* (Kraft, 2007)	6 y
EU-28 electricity price for non-household consumers, second half 2017, *ElP* (Eurostat, 2018)	0.16 \$ kWh^{-1}
Annual operation factor, *OF* (Zarca et al., 2018)	8000 h y^{-1}
Global pumping system efficiency, η (Vince et al., 2008)	80 %

658

659

660 **Table 4**. Integration with NF90 membrane optimization results.

PFHxA removal	***2-log***			***3-log***			***4-log***		
Number of stages in the membrane cascade	**1**	**2**	**3**	**1**	**2**	**3**	**1**	**2**	**3**
Membrane stage 1 area, A_1 (m^2)	28.1	14.0	12.4	2.6	16.0	14.0	2.6	24.8	15.4
Membrane stage 2 area, A_2 (m^2)		10.4	9.2		11.8	10.4		14.4	11.4
Membrane stage 3 area, A_3 (m^2)			9.2			10.3			11.3
Anode electrode area, A_e (m^2)	3.9	1.3	1.4	13.7	1.9	2.0	18.3	2.9	2.6
Pre-concentration time, t_{PC} (h)	4.0	12.6	14.2	0.0	11.0	12.6	0.0	9.0	11.5
Electrolysis time, t_{ELOX} (h)	36.0	27.4	25.8	40.00	29.0	27.4	40.0	31.0	28.5
Total annual cost, *TC* ($\$ y^{-1}$)	2.6E+04	1.3E+04	1.4E+04	7.8E+04	1.7E+04	1.8E+04	1.0E+05	2.3E+04	2.2E+04
Total specific cost, *TSC* ($\$ m^{-3}$)	12.9	6.4	7.2	39.0	8.3	9.1	51.0	11.7	10.9
Savings (%)	51.3	75.8	72.7	-	78.5	76.3	-	76.9	78.4

661

662

663 **Table 5**. Integration with NF270 membrane optimization results.

PFHxA removal	***2-log***			***3-log***			***4-log***		
Number of stages in the membrane cascade	**1**	**2**	**3**	**1**	**2**	**3**	**1**	**2**	**3**
Membrane stage 1 area, A_1 (m^2)	2.6	11.7	10.0	2.6	37.0	11.5	2.6	2.7	10.2
Membrane stage 2 area, A_2 (m^2)		9.4	8.0		10.2	9.2		2.6	36.9
Membrane stage 3 area, A_3 (m^2)			7.6			8.7			7.5
Anode electrode area, A_e (m^2)	9.1	1.5	1.4	13.7	11.4	2.0	18.3	18.3	3.2
Pre-concentration time, t_{PC} (h)	0.0	10.4	12.9	0.0	4.1	11.2	0.0	0.0	13.0
Electrolysis time, t_{ELOX} (h)	40.0	29.6	27.1	40.0	35.9	28.8	40.0	40.0	27.1
Total annual cost, *TC* ($ y^{-1})	5.4E+04	1.3E+04	1.3E+04	7.8E+04	7.0E+04	1.8E+04	1.0E+05	1.0E+05	2.7E+04
Total specific cost, *TSC* ($ m^{-3})	26.9	6.6	6.7	39.0	35.2	8.8	51.0	51.4	13.7
Savings (%)	-	75.0	74.7	-	8.9	77.2	-	-	72.9

664

665

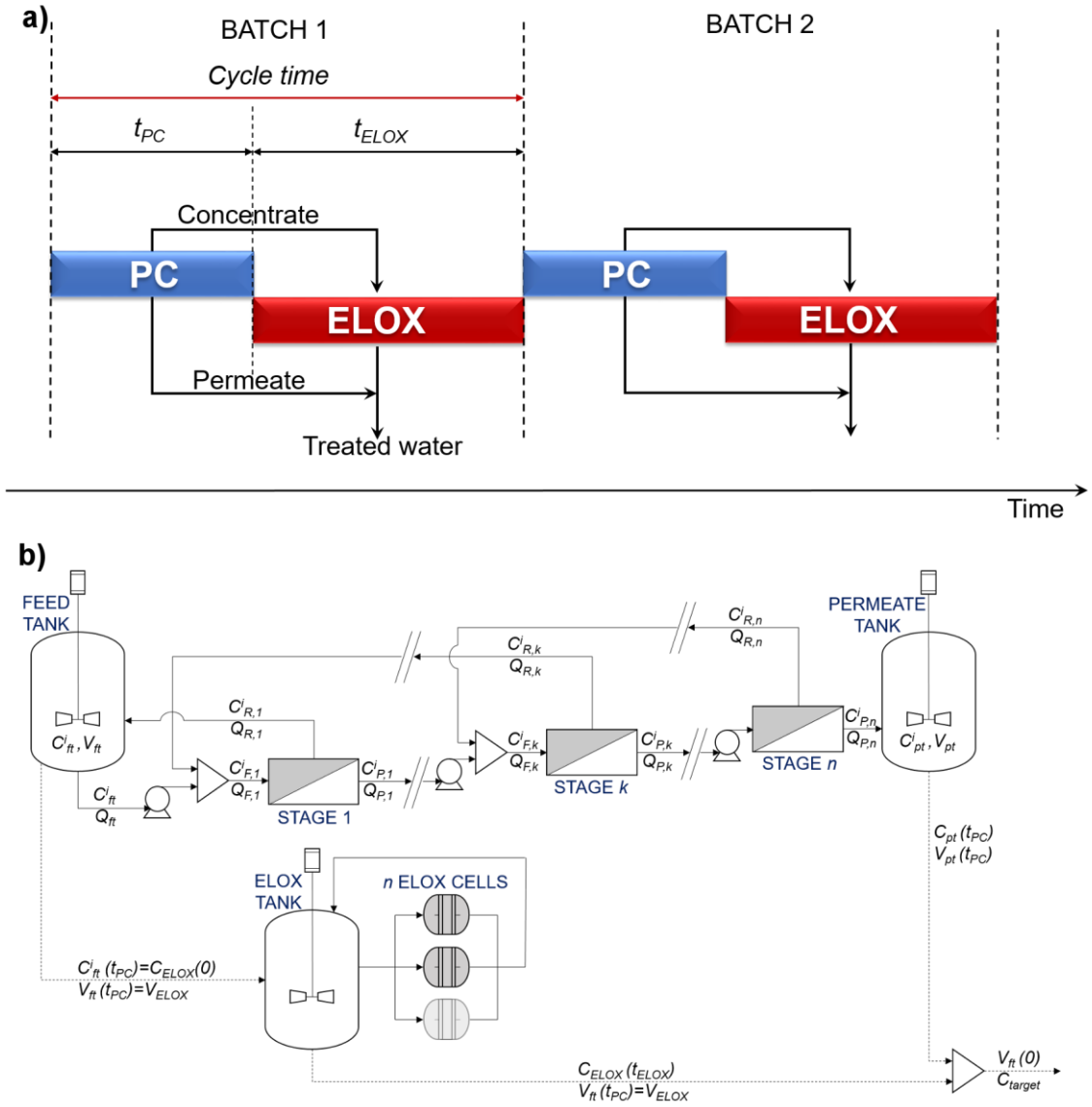

666

667 **Fig. 1.** Global scheme of the multistage countercurrent cascade membrane pre-concentration (PC)
668 coupled to electrooxidation (ELOX) system. a) Gantt-based chart for batch scheduling, b) detailed
669 process flowsheet.

670

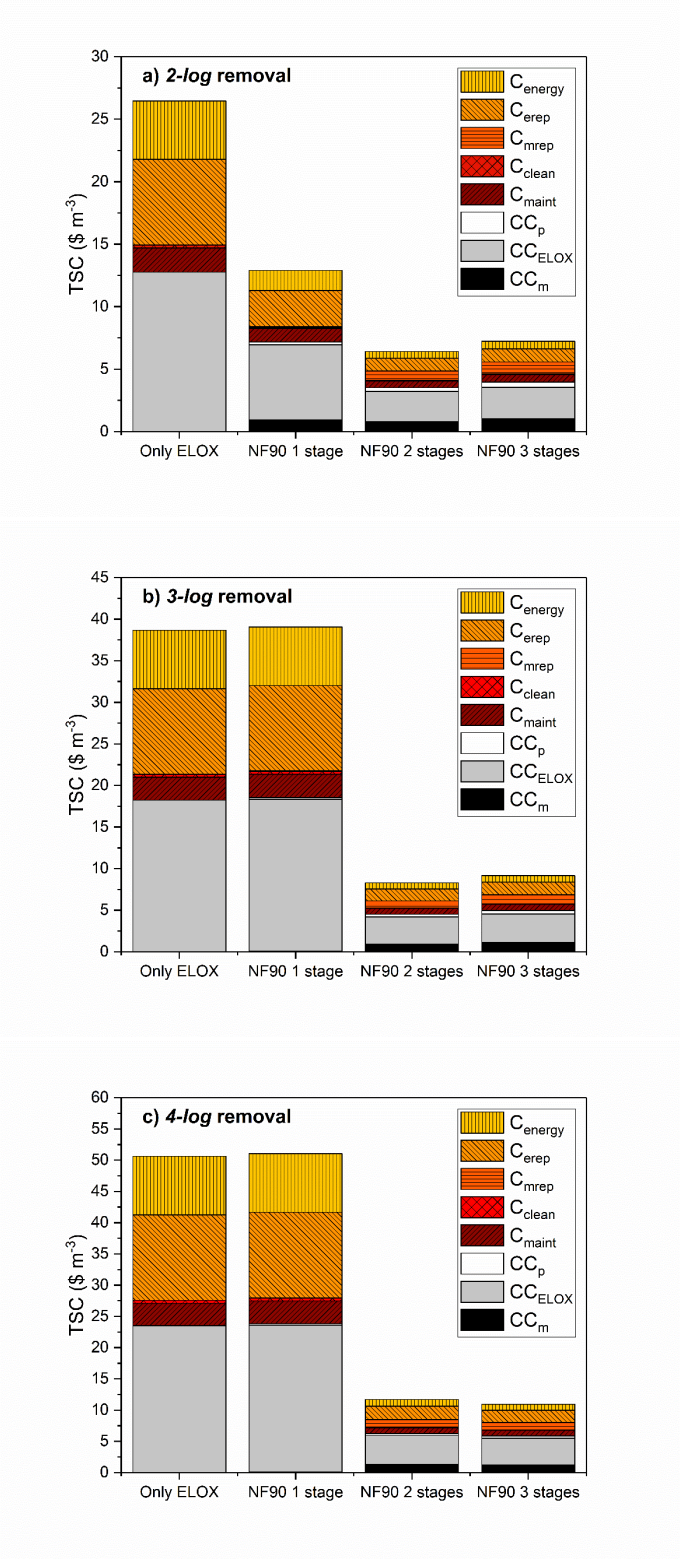

671 **Fig. 2.** Comparison of the CAPEX (CC) and OPEX (C) costs distribution for the 1, 2 and 3 NF90
672 membrane stages coupled to ELOX and the application of ELOX without pre-concentration for
673 different PFHxA abatement targets: 2-log, 3-log and 4-log.

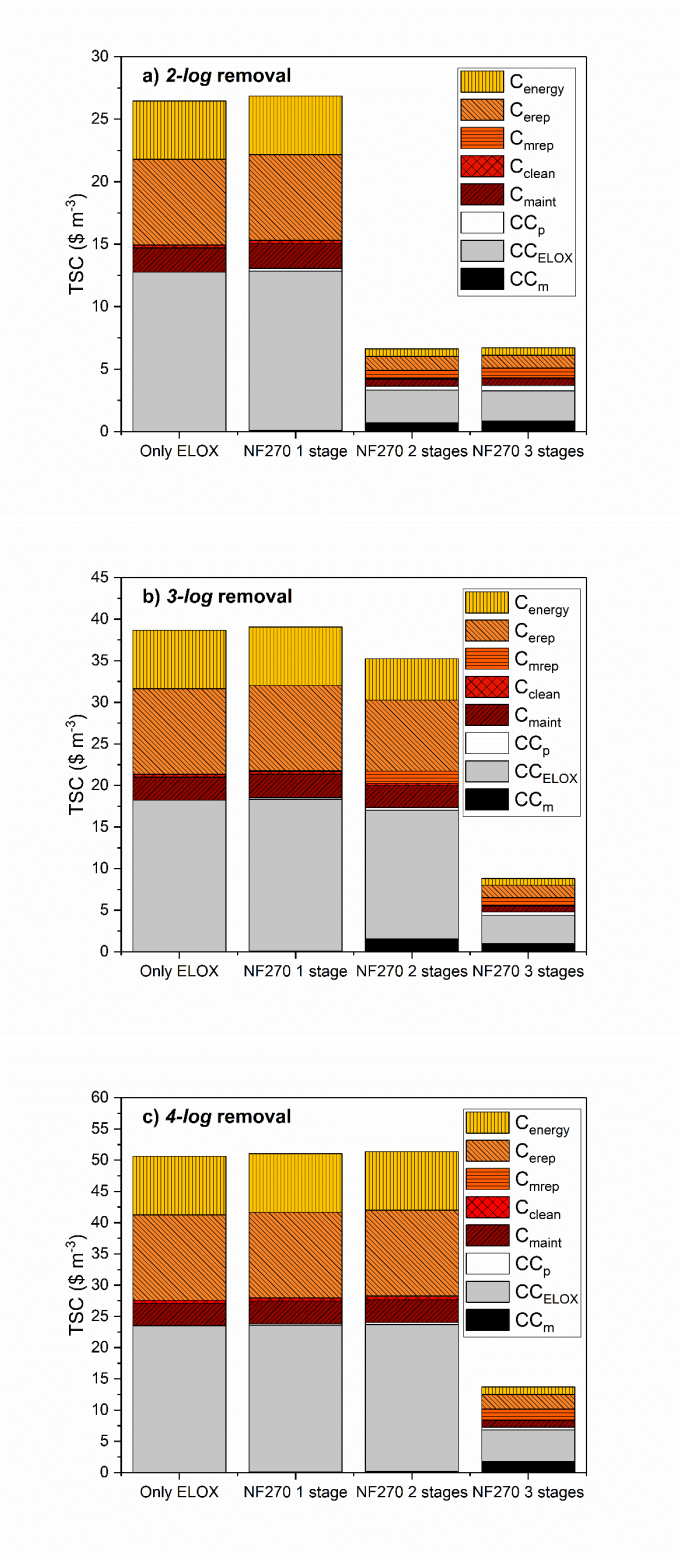

674 **Fig. 3.** Comparison of the CAPEX (CC) and OPEX (C) costs distribution for the 1, 2 and 3 NF270
675 membrane stages coupled to ELOX, and application of ELOX without pre-concentration for different
676 PFHxA abatement targets: 2-log, 3-log and 4-log.

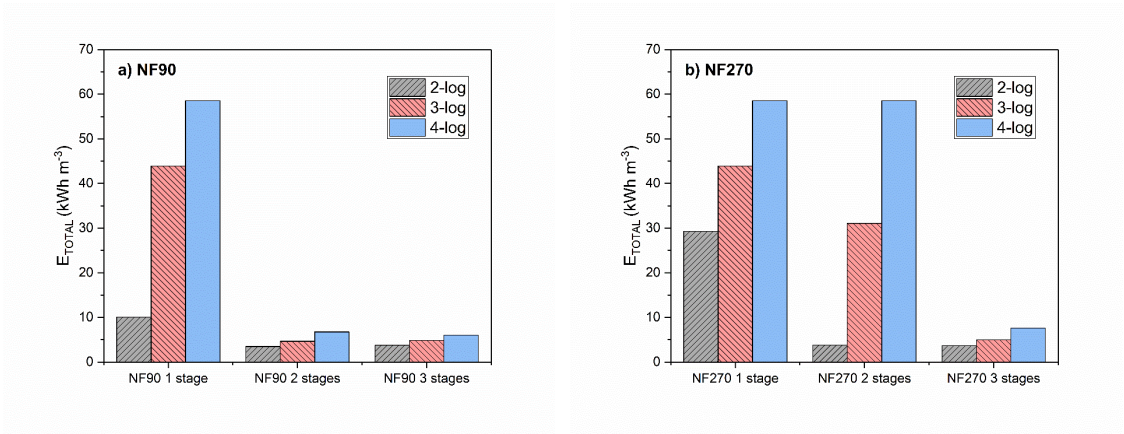

677 **Fig. 4.** Optimal total energy consumption of the hybrid process using the NF90 and NF270 membranes

678 for the different PFHxA abatement targets.

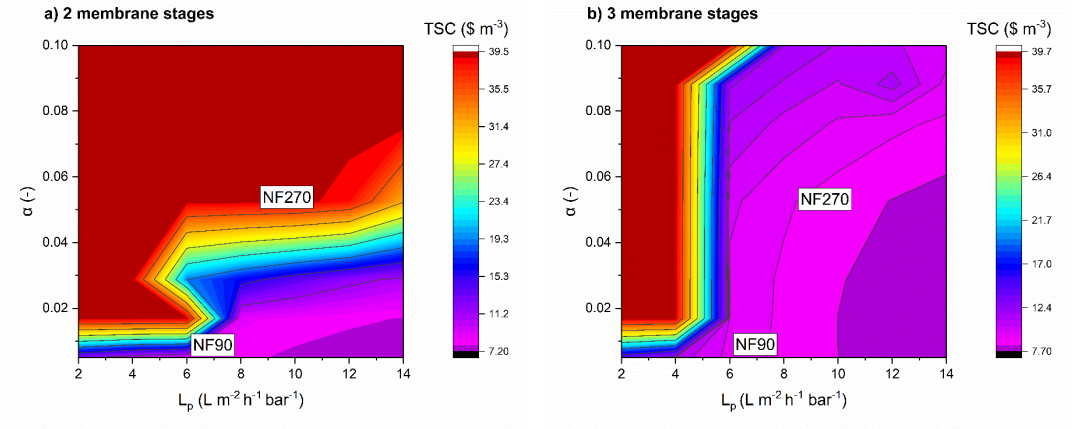

Fig. 5. Influence of the membrane properties on the total cost objective function for a *3-log* PFHxA abatement. (a) 2 membrane stages and (b) 3 membrane stages.

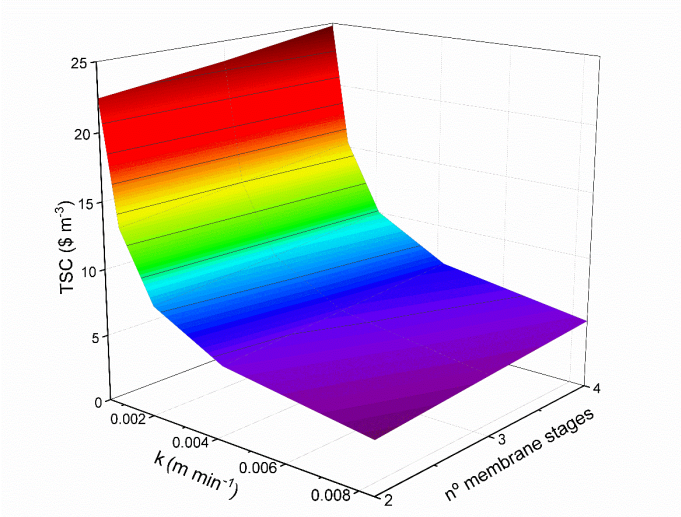

Fig. 6. Influence of the PFHxA degradation constant (k_{PFHxA}) on the total cost objective function for a *3-log* PFHxA abatement and different number of membrane stages. Integration with the NF90 membrane.